JOURNAL OF CATALYSIS 139, 304–321 (1993)

Oxidative Coupling of Methane over Alkali-Metal-Compound-Promoted Zirconia Catalysts

ASHRAF Z. KHAN AND ELI RUCKENSTEIN[1]

Department of Chemical Engineering, State University of New York at Buffalo, Buffalo, New York 14260

Received June 26, 1992; revised September 4, 1992

Upon promoting ZrO_2 with alkali metal compounds (chlorides, nitrates, carbonates, or acetates), effective catalytic systems are obtained which are more active, selective, and stable with time-on-stream than unpromoted ZrO_2 or unsupported promoter compounds at 750°C, P_{CH_4} = 243.2 Torr, CH_4/O_2 = 4, and a space velocity of 7500 $cm^3\ g^{-1}\ h^{-1}$. The performance of the catalysts is found to strongly depend on the nature of the alkali salt, the promoter content, the method of catalyst preparation, and the reaction conditions (temperature, partial pressures, CH_4/O_2 ratio, and contact time). The most effective catalytic system is obtained with Na^+–ZrO_2–Cl^- prepared via the sol–gel method, which leads to a methane conversion of 13.8 mol%, total C_2 selectivity of 77 mol% (C_2 yield 10.6%), and an ethylene-to-ethane ratio of 3.3 for at least 30 h under the aforementioned conditions and atmospheric pressure. Addition of carbon tetrachloride as a source of chlorine species to the feedstream improves the performance of the catalyst and its stability with time-on-stream. In the latter case, a CH_4 conversion of 22.0% and a C_2 yield of 17.5% with a C_2H_4/C_2H_6 molar ratio of 2.7 are obtained at a space velocity of 3750 $cm^3\ g^{-1}\ h^{-1}$. In contrast, Na^+–ZrO_2–Cl^- prepared via impregnation, gel-precipitation, physical mixing, or ion-exchange, and the Li-, K-, Rb-, or CsCl-promoted ZrO_2 catalysts prepared by any of the above methods, were less effective, even upon the addition of carbon tetrachloride to the feedstream. The relatively high performance of Na^+–ZrO_2–Cl^- (sol–gel) is attributed to the incorporation of Na^+Cl^- into the ZrO_2 matrix, the exposure of an appreciable amount of Na^+ and Cl^- on the surface, and the increase in basicity and base strength. The relationship between the catalytic performance and the physico-chemical characteristics of the catalysts revealed by XRD, XPS, and basicity (stepwise thermal desorption of CO_2) measurements is explored.

INTRODUCTION

During the past few years, an intensive search for effective catalysts for the oxidative coupling of methane (OCM) to C_2 hydrocarbons has shown that this important reaction occurs over many different types of catalysts, such as alkali and alkaline-earth metal compounds (*1–7*), rare-earth oxides (*8–11*), metal chlorides (*12–14*), oxychlorides (*15–17*), transition metal oxides (*18–22*), and many other different solid materials (*23, 24*). The oxides of the transition metals are generally more effective for the nonselective oxidation to the carbon oxides than for the selective oxidation to C_2 hydrocarbons. However, when promoted with alkali, or alkaline-earth metal oxides, halides, and oxyanions (such as phosphate), or present as composite partners, or used as supports, some transition metal oxides, notably MnO_2 and TiO_2, exhibit a considerable effect in the OCM process (*24*). Thus, the oxides of Mn, Ti, or Ni promoted with LiCl showed a high initial selectivity to ethylene, but this decreased sharply after 2 h of reaction (*25*). The addition of NaCl, instead of LiCl, to manganese oxides gave a better C_2 selectivity and catalyst stability that lasted for 8 h (*18*). When TiO_2 or ZrO_2 was used as a support for PbO (*26, 27*), the C_2 selectivity was much better than that over other supports.

Zirconium oxide is of interest both as a

[1] To whom correspondence should be addressed.

0021-9517/93 $5.00

support and a catalyst for a number of reactions (*28–29*). It has been reported (*29*) that a unique kind of interaction between the ZrO_2 support and the active phase gives rise to a specific activity and selectivity pattern. ZrO_2 surfaces possess both acidic and basic sites, as well as reducing and oxidizing abilities. Its acid and base strengths are weaker than those of TiO_2. The acidity and basicity of the catalysts and the supports are important factors in the selectivity of the coupling reaction (*24*). Usually, oxidative coupling catalysts operate at high temperatures (>700°C). Under such conditions, the acidic catalysts are effective for catalyzing oxidation of methane to carbon oxides. High C_2 selectivities are generally obtained with basic or less acidic supports. However, there exists the possibility of an involvement of an acid–base pair on the surface of rare-earth metal oxides in the abstraction of the H-atom from adsorbed methane (*30*).

Alkali-metal-halide-promoted TiO_2 showed some interesting results in the OCM process (*25*). This has stimulated us to investigate if alkali-compounds-promoted ZrO_2 are also effective in the OCM reaction. In the present work, we report on the catalytic performance of a number of alkali (chlorides, carbonates, nitrates, or acetates) promoted ZrO_2 in the OCM process. The effects of catalyst preparation procedure, the nature of the promoter compound used in the preparation of the promoted ZrO_2, the reaction conditions (temperature, partial pressures of CH_4 and O_2, contact time, CH_4/O_2 molar ratio, etc.), and the physical properties of the systems on the catalyst performance are presented. In addition, the influence of carbon tetrachloride (CTC) in the feedstream is examined. The addition of carbon tetrachloride to the feed-stream of OCM over SiO_2-supported alkali oxides was found to be beneficial in the recent study (*31*), but the long-term effect of such an addition was not studied. Although the methane conversion and the C_2 selectivity are generally increased in the presence of CTC, the extent of the increase is shown to be very much dependent on the nature of the promoter present in the promoted zirconia catalyst. We show that the Na^+Cl^--promoted ZrO_2, prepared via the sol–gel method, behaves as an effective system for the OCM process.

EXPERIMENTAL

Catalyst Preparation

Aldrich supplied powdered ZrO_2 (99% purity), TiO_2 (99%), MgO (99+%), high-surface-area SiO_2 (grade 951), $ZrO(NO_3)_2 \cdot x H_2O$ (96%), $Zr(OC_2H_5)_4$ (97%), alkali metal chlorides (99%), nitrates (99%), carbonates (99%), acetates (99%), NH_4Cl, CCl_4, C_2H_5OH, and double-distilled H_2O were used as reagents. The catalysts were prepared by impregnation of ZrO_2 with an aqueous solution of alkali metal chloride, nitrate, carbonate, or acetate at 80–85°C followed by drying overnight at 120°C, calcination in air at 750°C for 15 h, powdering, pressing, and crushing to 80-mesh particle sizes. In addition, the alkali-metal-chloride-promoted zirconia catalysts were prepared by four other methods: (i) gel-precipitation, (ii) physical mixing, (iii) ion-exchange, and (iv) sol–gel. The initial content of alkali metal chloride used in the preparation of the catalyst was 20 mol%. No attempt was made to analyze the elemental composition of the prepared catalysts.

In the gel-precipitation method, an aqueous solution of NaCl was added to a solution of zirconyl nitrate having a pH of 4–5. To this mixture, a solution of Na_2CO_3 was introduced dropwise under vigorous stirring. This was followed by filtering, washing, drying, and calcination. The final yield was 90%. The physical mixing method comprised grinding an appropriate amount of powdered NaCl and ZrO_2 followed by pressing, crushing, sieving, and calcination as above. In the ion-exchange method, which is similar to that reported in Ref. (*32*), the catalysts were prepared starting from an aqueous slurry which contained ZrO_2, $NaNO_3$, and NH_4Cl followed by drying, calcination, powdering, pressing, and crush-

ing as above. The latter catalyst is denoted Na^+–ZrO_2–Cl^- (i-e). In the sol–gel procedure, which is similar to that employed recently for the preparation of MgO and Li^+–MgO–Cl^- (*33, 34*), a slurry of zirconium ethoxide in ethanol was prepared in the presence of carbon tetrachloride, resulting in the incorporation of chlorine into the alkoxide. To the alkoxide slurry, $NaNO_3$ in carbon tetrachloride was added, and the resulting mixture was refluxed at 40°C followed by dropwise addition of distilled water. The resulting gel was separated by evaporating the solvent in a vacuum oven followed by drying and calcination as above. The resulting catalyst is denoted Na^+–ZrO_2–Cl^- (s–g). The incorporation of chlorine into ZrO_2 surface, both in the ion-exchange and sol–gel methods, was confirmed by XPS.

Catalyst Screening and Product Analysis

The methane coupling reactions were performed at 650–800°C under atmospheric pressure by cofeeding the reaction gases (P_{CH_4} = 243.2, P_{O_2} = 60.8, P_{He} = 456.0 Torr, and CH_4/O_2 = 4) into a high-purity alumina tube reactor heated by a single zone electric furnace. The details have been reported previously (*35*). The total gas flow was 25 ml/min (NTP), giving rise to a space velocity of 7500 $cm^3 g^{-1} h^{-1}$. In some of the runs, carbon tetrachloride (CTC) was introduced into the feedstream by bubbling a separate flow of helium through CCl_4 held at −40°C. The vapor pressure (10 Torr) of the additive was achieved by maintaining the temperature of the container at −40°C. Under the conditions employed, the purely homogeneous gas phase reactions produced less than 1% methane conversion. The product effluents, after separated from water, were sampled on-line using an automatic 10-port sampling valve and analyzed simultaneously with a dual detector (TCD and FID) GC (PE Sigma 2000) fitted with three different columns and attached to a PE 3600 data station. A Chromosorb 102 column (6 ft × $\frac{1}{8}$ in, 25° isothermal) was used to analyze O_2, CH_4, CO_2, C_2H_4, C_2H_6, and residual H_2O (if any), a molecular sieve 5A column (6 ft × $\frac{1}{8}$ in, 25° isothermal) to separate O_2, N_2, CH_4, and CO, and a Porapak T column (6 ft × $\frac{1}{8}$ in, programmed 25–140°C) to analyze CH_4, C_2H_4, C_2H_6, and C_3 hydrocarbons. Nitrogen was used as an internal standard. The response factors for the reactants and products were determined using certified calibration gases (Linde Division). The carbon mass balance was better than 95% in all experiments. No attempt was made to check the oxygen mass balance because of the condensation of H_2O before reaching the GC.

Catalyst Characterization

The catalysts were characterized by surface area measurements (BET method), X-ray diffraction analysis (XRD), X-ray photoelectron spectroscopy (XPS), and basicity/base strength distribution (stepwise thermal desorption of CO_2). The details of the XRD and the XPS methods have been described previously (*35*). The surface area of the samples was determined by the BET method using adsorption of nitrogen (gas) at liquid nitrogen temperature (Micromeritics 2100D). The basicity and base strength distribution on some selected catalysts (calcined in situ at 850°C in a flow of helium for 15 h) were determined by the stepwise thermal desorption (STD) of CO_2 with evolved gas analysis by a GC–MS according to a described method (*30*). The STD of CO_2 was carried out by desorbing the CO_2 chemisorbed at 50°C on the catalyst (1.0 g packed in an alumina reactor) in the flow of He (20 cm^3/min) by heating it from 50 to 850°C in a number of successive temperature steps (50–150°C, 150–300°C, 300–500°C, 500–700°C, and 700–850°C) at a heating rate of 10°C per min. When the maximum temperature of the respective step was attained, it was held at that temperature until no additional CO_2 desorbed (about 15 min). The chemisorption of high purity CO_2 (99.995%) was carried out by injecting successive pulses of 100 μl through a 6-port sampling valve until saturation of

the surface was achieved. The amount of CO_2 desorbed in each step was determined using a TC detector suitably calibrated. A known amount of La_2O_3 was used for calibration by comparing the results with reported values (*30*).

RESULTS

Catalytic Performance

The major products of catalytic methane coupling were C_2H_6, C_2H_4, CO_2, CO, and H_2O. In the presence of CTC, in addition to those products some C_3 hydrocarbons and CH_3Cl were detected. Pure ZrO_2 has a low activity for methane (conversion 2.4%), the carbon oxides (selectivity 82%) being the dominant products. When ZrO_2 is promoted with alkali metal compounds (chlorides, carbonates, nitrates or acetates), both the CH_4 and O_2 conversions are noticeably increased (Table 1). The C_2 selectivities and ethylene-to-ethane ratios, however, depend on the nature of the promoter compound. The Na-containing promoters produced the best systems followed by those of Li, while the K-, Rb-, and Cs-containing promoters showed low performances. In general, the alkali-metal-chloride-promoted ZrO_2 catalysts were better than the carbonate-, nitrate-, or acetate-promoted catalysts in terms of methane conversion, C_2 selectivity and, particularly, ethylene-to-ethane molar ratio. Of all the alkali-metal-chloride-promoted catalysts, prepared via impregnation, only Na^+Cl^--promoted ZrO_2 showed a noticeable C_2 selectivity (60%) with a high ethylene-to-ethane ratio (2.2). For this reason, the performance of Na^+–ZrO_2–Cl^- (impregnation) was compared with those of Na^+–MgO–Cl^-, Na^+–SiO_2–Cl^-, and Na^+–TiO_2–Cl^-, prepared via impregnation, and the results are presented in Table 2. The methane conversions over Na^+–ZrO_2–Cl^- and Na^+–MgO–Cl^- are comparable, but the C_2 selectivity is somewhat higher over the former catalyst. This makes the C_2 yield higher over Na^+–ZrO_2–Cl^- than over Na^+–MgO–Cl^-. The ethylene-to-ethane ratio is also higher over the former catalyst than over the latter one. Under the same conditions, the performances of Na^+–SiO_2–Cl^- and Na^+–TiO_2–Cl^- were very low, although their surface areas were much higher than that of Na^+–ZrO_2–Cl^- (Table 2).

Once the suitability of the alkali-metal-chloride-promoted ZrO_2 catalysts was established, they were prepared by five different methods. The catalytic results obtained are presented in Table 3. The highest CH_4 conversion, C_2 selectivity, C_2 yield, and ethylene-to-ethane ratio were obtained over the catalysts prepared by the sol–gel method. Thus, after 1 h of reaction, the CH_4 conversion over Na^+–ZrO_2–Cl^- (s–g) was 13.8 mol%, C_2 selectivity 77.0 mol%, C_2 yield 10.6%, and the ethylene-to-ethane ratio 3.3. These are the highest values ever reported for any ZrO_2-containing catalyst in the OCM process. The performances of Na^+–ZrO_2–Cl^- prepared via impregnation, gel-precipitation, mixing, or ion-exchange were close to each other and much lower than that of the sol–gel process. Particularly, the C_2 yield was less than half that of the sol–gel method. The surface area of Na^+–ZrO_2–Cl^- (s–g) was somewhat higher than those prepared in the other procedures, but close to that of ZrO_2. Under the same conditions, Li^+–ZrO_2–Cl^-, K^+–ZrO_2–Cl^-, Rb^+–ZrO_2–Cl^-, and Cs^+–ZrO_2–Cl^- (also prepared via the sol–gel method) showed lower CH_4 conversion and, most notably, much lower C_2 selectivity, C_2 yield, and ethylene-to-ethane ratio than those over Na^+–ZrO_2–Cl^- (s–g) (Table 3).

Since Na^+–ZrO_2–Cl^- prepared via the sol–gel method was found to be the most effective catalyst, further investigation was concentrated on this catalyst. Figure 1 illustrates the effect of the reaction temperature (650–800°C) on the oxidative coupling over Na^+–ZrO_2–Cl^- (s–g). With the increase in temperature, both the CH_4 and O_2 conversions increase, but the C_2 selectivity passes through a maximum at 750°C with an ethylene-to-ethane molar ratio of 3.3, whereas that to CO_x(x = 1, 2) starts rising above

TABLE 1

Surface Area and Effect of Alkali-Metal-Compound-Promoted Zirconia Prepared via an Impregnation Method on the OCM

Catalyst	Surface area (m^2/g)	Conversion (mol%)		Selectivity (mol%)			C_2 Yield (%)	Ethylene/ ethane molar ratio
		Methane	Oxygen	Ethane	Ethylene	Carbon oxides		
ZrO_2	8.6	2.4	28.0	14.6	3.4	82.0	0.43	0.23
Na^+Cl^-	2.2	2.9	30.0	11.0	13.0	76.0	0.70	1.18
Li^+–ZrO_2–Cl^-	4.4	4.8	39.2	14.0	18.0	68.0	1.53	1.28
Na^+–ZrO_2–Cl^-	4.8	8.7	45.0	19.0	41.0	40.0	5.22	2.15
K^+–ZrO_2–Cl^-	4.0	4.8	41.0	13.0	15.0	72.0	1.34	1.15
Rb^+–ZrO_2–Cl^-	5.8	4.2	38.0	13.0	14.0	73.0	1.13	1.07
Cs^+–ZrO_2–Cl^-	6.5	5.0	40.0	14.0	16.0	70.0	1.50	1.14
Li^+–ZrO_2–CO_3^-	4.2	4.6	44.0	18.0	13.0	69.0	1.42	0.72
Na^+–ZrO_2–CO_3^-	4.5	8.2	50.0	31.0	24.0	45.0	4.51	0.77
K^+–ZrO_2–CO_3^-	4.8	4.4	48.0	17.0	9.0	74.0	1.14	0.52
Rb^+–ZrO_2–CO_3^-	5.2	4.2	46.0	16.0	9.0	75.0	1.05	0.56
Cs^+–ZrO_2–CO_3^-	5.0	4.6	48.0	18.0	10.0	72.0	1.28	0.55
Li^+–ZrO_2–NO_3^-	4.5	5.0	46.0	20.0	12.0	68.0	1.60	0.60
Na^+–ZrO_2–NO_3^-	5.2	8.5	55.4	31.0	21.0	48.0	4.42	0.67
K^+–ZrO_2–NO_3^-	5.4	4.7	50.2	21.0	10.0	69.0	1.45	0.47
Rb^+–ZrO_2–NO_3^-	4.6	4.8	45.8	18.0	10.0	72.0	1.34	0.55
Cs^+–ZrO_2–NO_3^-	5.4	5.5	48.0	19.0	12.0	69.0	1.70	0.63
Li^+–ZrO_2–Ac^-	5.0	4.9	48.4	17.0	13.0	70.0	1.47	0.76
Na^+–ZrO_2–Ac^-	5.4	8.6	53.2	31.0	24.0	45.0	4.73	0.77
K^+–ZrO_2–Ac^-	4.9	4.8	47.0	18.0	11.0	71.0	1.39	0.61
Rb^+–ZrO_2–Ac^-	5.3	4.3	48.0	17.0	12.0	71.0	1.24	0.70
Cs^+–ZrO_2–Ac^-	5.5	5.2	50.8	16.0	11.0	73.0	1.40	0.68

Note. Reaction conditions: temperature = 750°C, pressure = 1 atm, space velocity = 7500 $cm^3\ g^{-1}\ h^{-1}$, P_{CH_4} = 243.2 Torr, CH_4/O_2 = 4, and catalyst = 0.2 g; products measured after 1 h of reaction.

TABLE 2

Oxidative Coupling of Methane over Na^+Cl^--promoted Different Oxides Prepared via an Impregnation Method and Their Surface Areas

Catalyst	Surface area (m^2/g)	Conversion (mol%)		Selectivity (mol%)			C_2 Yield (%)	Ethylene/ ethane molar ratio
		Methane	Oxygen	Ethane	Ethylene	Carbon oxides		
Na^+–ZrO_2–Cl^-	4.8	8.7	45.0	19.0	41.0	40.0	5.22	2.15
Na^+–MgO–Cl^-	9.6	8.9	52.0	18.0	30.0	52.0	4.27	1.66
Na^+–SiO_2–Cl^-	360.0	3.3	41.2	14.0	16.0	70.0	1.00	1.14
Na^+–TiO_2–Cl^-	26.5	4.8	42.8	17.0	28.0	55.0	2.16	1.64

Note. Reaction conditions: as in Table 1; products measured after 1 h of reaction.

TABLE 3

Effect of Preparation Method of Alkali Metal Chloride Promoted Zirconia on the OCM and the Surface Area of the Catalysis

Catalyst	Surface area (m^2/g)	Conversion (mol%)		Selectivity (mol%)			C_2 Yield (%)	Ethylene/ ethane molar ratio
		Methane	Oxygen	Ethane	Ethylene	Carbon oxides		
				Sol–gel				
Li^+–ZrO_2–Cl^-	5.2	9.6	50.0	16.0	33.0	51.0	4.70	2.06
Na^+–ZrO_2–Cl^-	7.8	13.8	58.8	18.0	59.0	23.0	10.62	3.27
K^+–ZrO_2–Cl^-	5.8	7.0	51.0	14.2	20.0	65.8	2.40	1.42
Rb^+–ZrO_2–Cl^-	5.6	6.2	44.0	14.0	15.2	70.6	1.81	1.08
Cs^+–ZrO_2–Cl^-	7.0	6.8	50.4	13.0	20.0	67.0	2.24	1.53
				Impregnation				
Li^+–ZrO_2–Cl^-	4.4	4.8	39.2	14.0	18.0	68.0	1.53	1.28
Na^+–ZrO_2–Cl^-	4.8	8.7	45.0	19.0	41.0	40.0	5.22	2.15
K^+–ZrO_2–Cl^-	4.0	4.8	41.0	13.0	15.0	72.0	1.34	1.15
Rb^+–ZrO_2–Cl^-	5.8	4.2	38.0	13.0	14.0	73.0	1.13	1.07
Cs^+–ZrO_2–Cl^-	6.5	5.0	40.0	14.0	16.0	70.0	1.50	1.14
				Gel-precipitation				
Li^+–ZrO_2–Cl^-	5.0	6.4	44.0	16.0	22.0	62.0	2.43	1.37
Na^+–ZrO_2–Cl^-	4.2	8.8	48.8	14.0	41.0	45.0	4.84	2.92
K^+–ZrO_2–Cl^-	4.6	6.9	42.4	15.0	18.0	67.0	2.27	1.20
Rb^+–ZrO_2–Cl^-	5.2	5.0	42.0	16.0	16.0	68.0	1.60	1.00
Cs^+–ZrO_2–Cl^-	4.2	6.2	45.4	16.0	19.0	65.0	2.17	1.30
				Physical mixing				
Li^+–ZrO_2–Cl^-	3.8	3.4	34.0	14.0	16.0	70.0	1.02	1.14
Na^+–ZrO_2–Cl^-	4.5	7.8	49.0	15.0	35.0	50.0	3.90	2.33
K^+–ZrO_2–Cl^-	4.2	4.0	40.8	14.0	17.0	69.0	1.24	1.21
Rb^+–ZrO_2–Cl^-	5.0	3.8	38.0	13.0	15.0	72.0	1.06	1.15
Cs^+–ZrO_2–Cl^-	4.9	4.8	42.0	14.0	22.0	64.0	1.72	1.57
				Ion-exchange				
Li^+–ZrO_2–Cl^-	5.4	4.0	41.4	17.0	23.0	60.0	1.60	1.35
Na^+–ZrO_2–Cl^-	6.4	8.2	45.0	19.0	46.0	35.0	5.33	2.42
K^+–ZrO_2–Cl^-	6.8	4.2	41.0	15.0	19.0	66.0	1.42	1.26
Rb^+–ZrO_2–Cl^-	7.4	4.8	40.2	13.0	17.0	70.0	1.44	1.30
Cs^+–ZrO_2–Cl^-	7.0	4.9	42.0	15.0	17.0	68.0	1.56	1.13

Note. Reaction conditions: as in Table 1; products measured after 1 h of reaction.

750°C (Fig. 1a). In the presence of CTC in the feedstream, both the CH_4 conversion and C_2 selectivity increase further. The highest C_2 yield (15.6%) was obtained, however, at 750°C due to the highest C_2 selectivity (Fig. 1b).

Figure 2 shows the effect of promoter content (Na^+Cl^-) on the OCM over promoted ZrO_2 at 750°C. The highest CH_4 conversion (13.8%) and C_2 selectivity (77%) were obtained over 20 mol% Na^+Cl^- promoted ZrO_2 (Fig. 2a). Further increases in Na^+Cl^- composition decreased the CH_4 conversion and/or the C_2 selectivity. Upon introduction of CTC to the feedstream, both the CH_4 conversion and C_2 selectivity increased but the 20% Na^+Cl^--promoted ZrO_2 in the presence of CTC remained the most effective catalyst in terms of C_2 yield (15.6%) and ethylene-to-ethane ratio (3.6) (Fig. 2b).

In order to determine the effect of the pseudo-contact time or the reciprocal space velocity (W/F), the amount of catalyst (W) was varied while the flow rate (F) was held

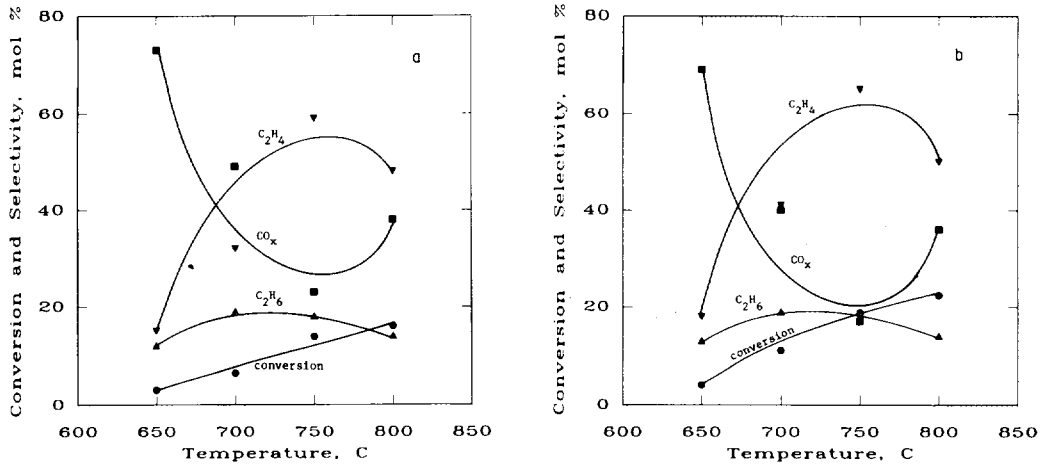

FIG. 1. Effect of reaction temperature on methane conversion (●) and selectivity to ethane (▲), ethylene (▼), and carbon oxides (■) over Na^+–ZrO_2–Cl^- (s–g). Conditions: pressure = 1 atm, space velocity = 7500 $cm^3\ g^{-1}\ h^{-1}$, $CH_4/O_2 = 4$, $P_{CH_4} = 243.2$ Torr, and catalyst = 0.2 g: (a) in the absence of CTC and (b) in the presence of CTC.

constant. Figure 3 illustrates the effect of the reciprocal space velocity (W/F) on the methane and oxygen conversions and the yields of various carbon products over Na^+–ZrO_2–Cl^- (s–g) at 750°C. At a short pseudo-contact time (low catalyst content), the total C_2 yield (Fig. 3a) is 3.5 times higher than that of the carbon oxides due to the high C_2 selectivity. With increasing pseudo-contact time, the total C_2 yield passes through a maximum (10.6%) at $W/F = 0.48$ g · s/ml, whereas that of carbon oxides continues to increase. Both the methane and O_2 conversions increase with W/F (Fig. 3a).

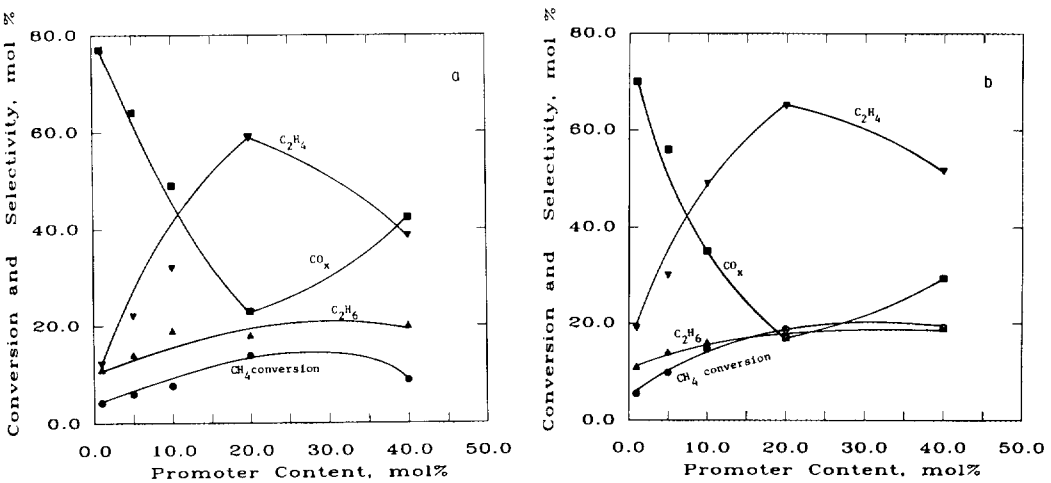

FIG. 2. Effect of promoter content on methane conversion (●) and selectivity to ethane (▲), ethylene (▼), and carbon oxides (■) over Na^+–ZrO_2–Cl^- (s–g). Conditions: pressure = 1 atm, temperature = 750°C, space velocity = 7500 $cm^3\ g^{-1}\ h^{-1}$, $CH_4/O_2 = 4$, $P_{CH_4} = 243.2$ Torr, and catalyst = 0.2 g: (a) in the absence of CTC and (b) in the presence of CTC.

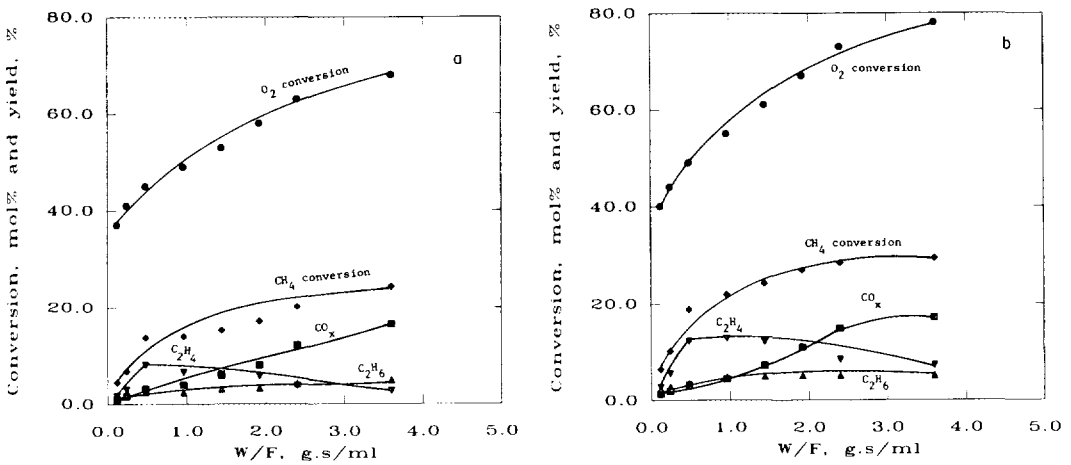

FIG. 3. Effect of reciprocal space velocity (W/F (pseudo-contact time) on conversion of methane (◆), oxygen (●), and carbon product yield of ethane (▲), ethylene (▼), and carbon oxides (■) over Na^+–ZrO_2–Cl^- (s–g). Conditions: pressure = 1 atm, temperature = 750°C, total flow = 25 ml/min (NTP), $CH_4/O_2 = 4$, $P_{CH_4} = 243.2$ Torr: (a) in the absence of CTC and (b) in the presence of CTC.

The ethylene-to-ethane ratio grows initially, but above $W/F = 0.48$ g · s/ml it decreases due to the decrease in ethylene selectivity; the selectivity to ethane remains almost constant. In the presence of CTC, the yields and the CH_4 and O_2 conversions were somewhat higher (Fig. 3b) than those in the absence of CTC. The change patterns for the yields and conversions with W/F were, however, similar to those observed in the absence of CTC. A C_2 yield as high as 17.5% with an ethylene/ethane = 2.7 was obtained at $W/F = 0.96$ g · s/ml. This is the highest C_2 yield obtained in the present study.

Figure 4 presents the change in selectivity with methane conversion obtained by varying W/F. At low methane conversion (4.5%), the C_2 selectivity is quite high (78%); it decreases noticeably with the increase in methane conversion (Fig. 4a). The ethylene/ethane ratio, after passing through a maximum at a conversion of 13.8 mol%, also decreases with increasing methane conversion. In the presence of CTC, a similar trend was observed, but with enhanced values for methane conversion and C_2 selectivity (Fig. 4b), the selectivity to CO_x ($x = 1, 2$) being somewhat lower than in Fig. 4a.

Figure 5 presents the effect of the partial pressure of methane on methane conversion and C_2 selectivity over Na^+–ZrO_2–Cl^- (s–g) at 750°C while holding the partial pressure of oxygen constant at 60.8 Torr. The partial pressures of methane were changed such that the methane-to-oxygen ratios varied between 1 and 8 in integer numbers. At a low partial pressure of methane ($CH_4 : O_2 = 1$), both the methane and oxygen conversions were quite high but the total C_2 selectivity was only 3 mol% (Fig. 5a). With the increase in the methane partial pressure ($CH_4 : O_2$ increasing), the methane conversion decreases but the C_2 selectivity increases accompanied by a decrease in CO_x ($x = 1, 2$) selectivity. The highest C_2 yield (10.6%) is obtained at a methane partial pressure of 243.2 Torr ($CH_4 : O_2 = 4$). Increasing the methane partial pressure further decreases the C_2 yield due to the drastic decrease in methane conversion. At the highest methane partial pressure, however, the ethylene-to-ethane molar ratio becomes as high as 3.7. In the presence of CTC in the feedstream, similar trends in methane conversion, C_2 selectivity and ethylene-to-ethane ratio were observed but with enhanced val-

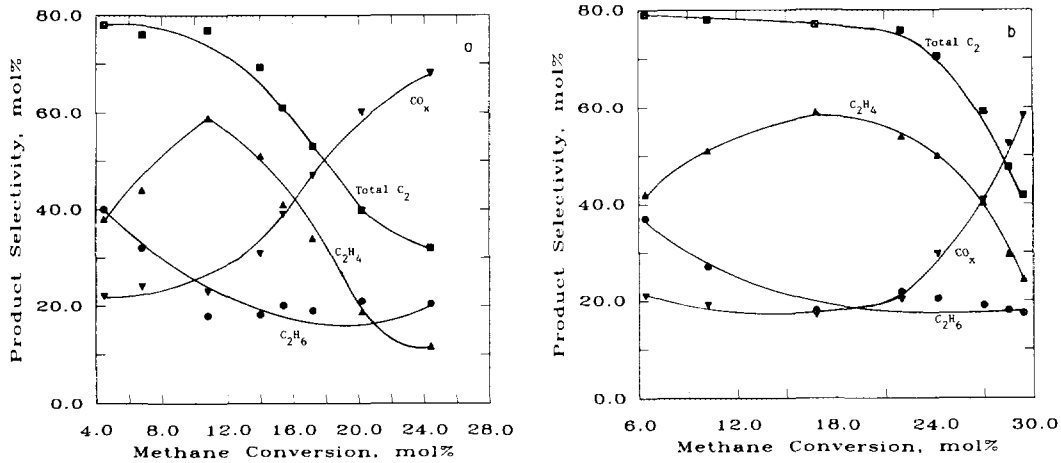

FIG. 4. Change in product selectivity with methane conversion over Na^+–ZrO_2–Cl^- (s–g): ethane (●), ethylene (▲), total C_2 hydrocarbons (■), and carbon oxides (▼). Conditions: pressure = 1 atm, temperature = 750°C, P_{CH_4} = 243.2 Torr, CH_4/O_2 = 4, and space velocity = 7500 $cm^3\ g^{-1}\ h^{-1}$: (a) in the absence of CTC and (b) in the presence of CTC.

ues (Fig. 5b). A C_2 yield as high as 15.6% is obtained at P_{CH_4} = 243.2 Torr ($CH_4 : O_2$ = 4) and P_{CTC} = 10 Torr.

The effect of oxygen partial pressure, keeping the methane partial pressure constant at 243.2 Torr, was also examined such that the methane-to-oxygen ratio varied between 16 and 1 in integer numbers (Fig. 6). At a low partial pressure of oxygen (high $CH_4 : O_2$ ratio) the methane conversion is quite low (2.0%) but the C_2 selectivity is quite high (67%), with the ethylene-to-ethane ratio of 3.5 (Fig. 6a). This trend is similar to that observed at high methane partial

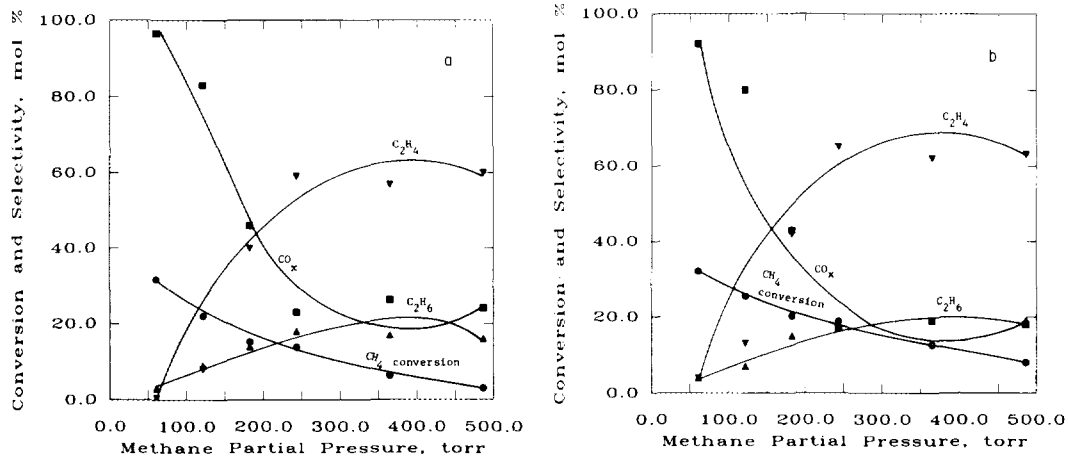

FIG. 5. Effect of partial pressure of methane on methane conversion (●) and selectivity to ethane (▲), ethylene (▼), and carbon oxides (■) over Na^+–ZrO_2–Cl^- (s–g). Conditions: pressure = 1 atm, temperature = 750°C, space velocity = 7500 $cm^3\ g^{-1}\ h^{-1}$, P_{O_2} = 60.8 Torr, and catalyst = 0.2 g: (a) in the absence of CTC and (b) in the presence of CTC.

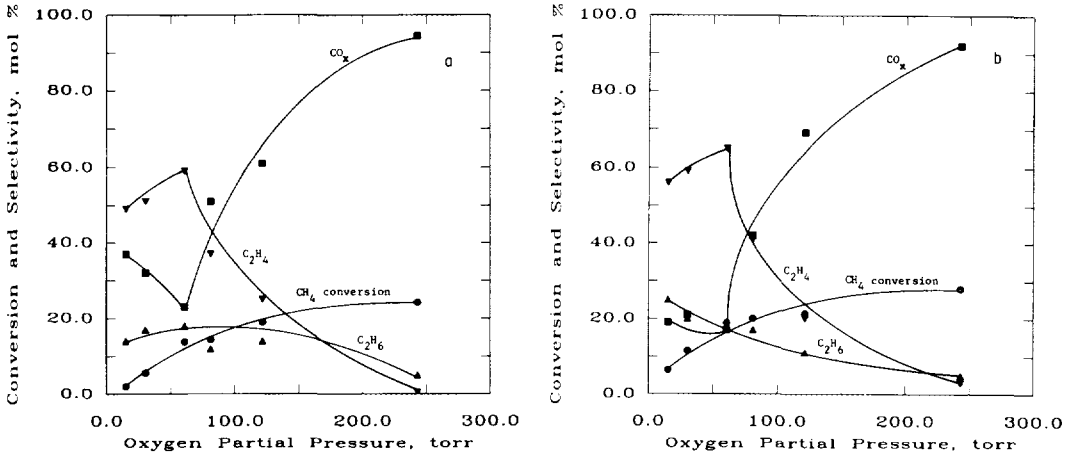

FIG. 6. Effect of partial pressure of oxygen on methane conversion (●) and selectivity to ethane (▲), ethylene (▼), and carbon oxides (■) over Na^+–ZrO_2–Cl^- (s–g). Conditions: pressure = 1 atm, temperature = 750°C, space velocity = 7500 $cm^3\ g^{-1}\ h^{-1}$, P_{CH_4} = 243.2 Torr, and catalyst = 0.2 g: (a) in the absence of CTC and (b) in the presence of CTC.

pressure in Fig. 5a. With the increase in oxygen partial pressure (lowering the methane-to-oxygen ratio), the methane conversion increases, but the C_2 selectivity passes through a maximum at 60.8 torr. At a high oxygen partial pressure, although the methane conversion increases, carbon oxides become the dominant products. When CTC was added to the feedstream, similar trends were observed but with enhanced values (Fig. 6b). The highest C_2 yield (15.6%) is obtained at P_{O_2} = 60.8 Torr ($CH_4 : O_2$ = 4) and P_{CTC} = 10 Torr.

The stability of the catalysts, prepared via the sol–gel method, with time-on-stream was also examined. The change in C_2 selectivity is presented in Fig. 7. For the Na^+–ZrO_2–Cl^- (s–g) catalyst, after a slight initial decrease, the C_2 selectivity is maintained at a high level (73%) for 30 h with the C_2H_4/C_2H_6 ratio constant at 3.1 (Fig. 7a). In contrast, other catalysts of the alkali series have much lower initial C_2 selectivities and show a noticeable decrease (around 30%) in C_2 selectivity during the same period. The C_2H_4/C_2H_6 ratio also exhibited some decrease. The methane conversion did not vary much for all these catalysts (only a variation of 5% was observed during the same period). When CTC was added to the feedstream, the enhanced C_2 selectivity over Na^+–ZrO_2–Cl^- (s–g) was maintained for a longer period (50 h) than for the other catalysts of the alkali series (Fig. 7b).

XRD Analysis

The alkali-metal-chloride-promoted ZrO_2 samples are crystalline compounds with diffraction lines less intense than those of the precursor materials. In general, the ZrO_2 lines are most prominent. No separate lines of the chlorides could be identified, perhaps due to the overlapping of some of the strongest lines with those of ZrO_2 or due to small crystallite sizes of the chlorides. The XRD profiles of Na^+–ZrO_2–Cl^- (*36*) prepared by four different methods are presented in Fig. 8. The samples prepared by impregnation, gel-precipitation, or ion-exchange showed almost identical lines (Figs. 8a–8c), which match well with those of the ZrO_2 (Baddeleyite) phase (*37*). The sample prepared via the sol–gel method exhibited some additional lines with *d*-spacing values of 5.40, 2.91, and 2.30 Å (Fig. 8d) which could not be assigned to any of the JCPDS database

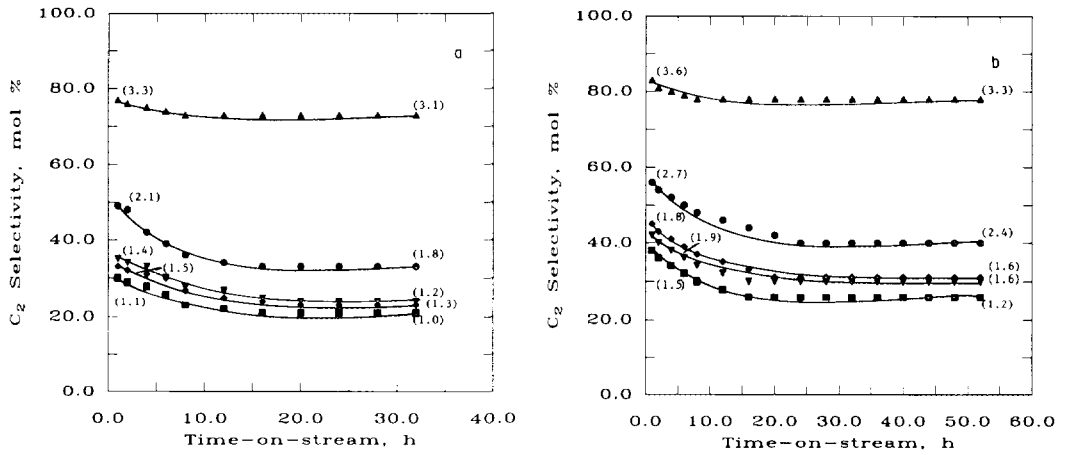

FIG. 7. Change in C_2 selectivity with time-on-stream over alkali metal chloride promoted zirconia (s–g). (The numbers in parentheses represent the ethylene-to-ethane ratios.) Conditions: pressure = 1 atm, temperature = 750°C, space velocity = 7500 $cm^3\ g^{-1}\ h^{-1}$, $CH_4/O_2 = 4$, $P_{CH_4} = 243.2$ Torr, and catalyst = 0.2 g: (●) Li^+–ZrO_2–Cl^-, (▲) Na^+–ZrO_2–Cl^-, (▼) K^+–ZrO_2–Cl^-, (■) Rb^+–ZrO_2–Cl^-, (◆) Cs^+–ZrO_2–Cl^-; (a) in the absence of CTC and (b) in the presence of CTC.

patterns for zirconium oxide, sodium chloride, or zirconium alkoxide. Presumably, a new unknown phase is formed during the sol–gel method. In addition, some major lines of ZrO_2 are broadened to some extent by the addition of Na^+Cl^- (Fig. 8d), suggesting that a certain amount of Na^+Cl^- is incorporated into the ZrO_2 matrix. Such a line-broadening effect was absent in the catalysts prepared by the other methods.

XPS Results

The electron-binding energies of the Na1*s* (1072.4 eV), Cl1*s* (197.0 eV), Zr3*d* (181.7 and 184.7 eV), O1*s* (529.6 and 532.5 eV), and C1*s* (285.0 and 289.9 eV) levels in the Na^+Cl^--promoted ZrO_2 samples are in agreement with the reported values (*38*). The C1*s* and O1*s* spectra which have two different binding energies only in the sample prepared via the sol–gel method provide evidence that multiple carbon and oxygen species are present on the surface of this catalyst. The higher binding energy of O1*s* is ascribed to the carbonate-type, whereas the lower value to the oxide-type oxygen (*35, 39*). For C1*s* the lower binding energy is ascribed to graphite or hydrocarbons and the higher to carbonates. In the samples prepared via other methods, multiple oxygen species were present only after reaction, but carbon was never present in multiple states.

The surface compositions of the elements present in Na^+–ZrO_2–Cl^- (*36*) prepared via impregnation, gel-precipitation, and sol–gel methods are presented in Table 4. The Na/Zr and Cl/Zr ratios depend on the method of preparation and are the largest for the sample prepared via the sol–gel method. Thus, the surface concentration of Na in the calcined sample prepared via the sol–gel method is 5–6 times greater than in those prepared via gel-precipitation and impregnation. The surface chlorine concentration also shows a 3–4-fold increase compared to those obtained via gel-precipitation and impregnation. The surface sodium concentration, which exceeds that of zirconium, increases to some extent after the catalytic reaction for Na^+–ZrO_2–Cl^- (s–g).

STD of CO_2

The basicity possessed by and the base strength distribution on the pure ZrO_2 and

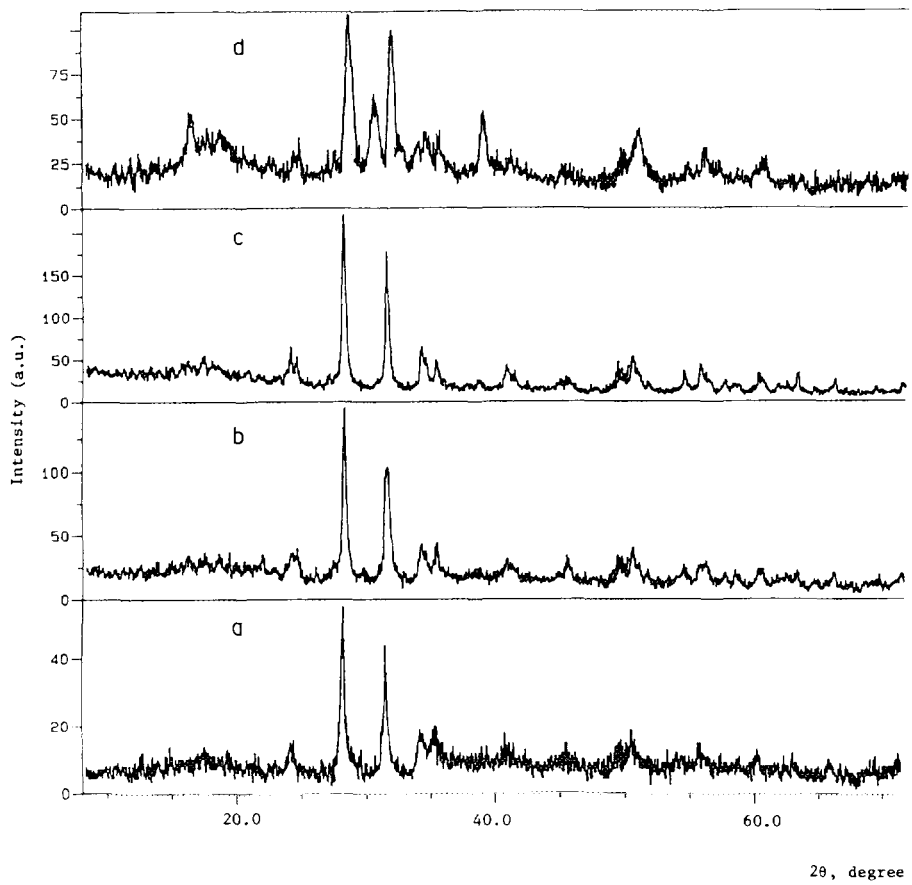

FIG. 8. XRD patterns of Na^+–ZrO_2–Cl^- prepared via four different methods after calcination at 750°C, 15 h: (a) impregnation, (b) gel-precipitation, (c) ion-exchange, and (d) sol–gel.

Na^+–ZrO_2–Cl^- prepared by five different methods and calcined *in situ* at 850°C in He flow under conditions close to those of the catalytic reaction have been determined by the STD of CO_2. Any contribution from volatile chlorine was eliminated by passing the effluent through a heptanol-liquid N_2 bath (−40°C). The base strength distribution on ZrO_2 and Na^+–ZrO_2–Cl^- is presented in Fig. 9. Each column represents the number of sites measured in terms of CO_2 desorbed during the corresponding temperature step. The strength of these sites is expressed in terms of the desorption temperature of CO_2. Evidently, pure ZrO_2 is an extremely weak base, as can be seen from the small amount of CO_2 chemisorbed and from its base strength distribution, which is quite low (Fig. 9a). This is consistent with Ref. (*28*) that ZrO_2 is a poor base and acid. Upon promoting ZrO_2 with Na^+Cl^-, the total basicity and base strength are noticeably increased. However, this increase greatly depends on the method of preparation. Na^+–ZrO_2–Cl^- prepared via the sol–gel method exhibits the highest total basicity (measured in terms of the CO_2 chemisorbed at 50°C) and a broad site energy distribution for their basic sites (Fig. 9f). The basicity possessed by the samples prepared by the other methods (Figs 9b–9e) occupies an intermediate position between that of pure

TABLE 4

Surface Composition of the Elements in Na^+–ZrO_2–Cl^- after Calcination and Calcination Plus Reaction Determined by XPS

Method of preparation	Pretreatment/ reaction conditions	Surface atomic ratio[a]		
		Na/Zr	Cl/Zr	O/Zr
Gel-precipitation	Calcined, 750°C, 15 h	0.32	0.03	2.53
Gel-precipitation	Calcined as above + reaction, 750°C, 30 h	0.49	0.05	4.11
Impregnation	Calcined, 750°C, 15 h	0.26	0.04	2.26
Impregnation	Calcined as above + reaction, 750°C, 30 h	0.40	0.06	3.75
Sol–gel	Calcined, 750°C, 15 h	1.61	0.12	4.73
Sol–gel	Calcined as above + reaction, 750°C, 30 h	1.90	0.17	5.11

[a] Calculated from the atomic concentration given by

$$C_x = \frac{I_x/S_x}{\Sigma_i I_i/S_i},$$

where I_x is the relative peak area of photoelectrons from element x and, S_x is the atomic sensitivity factor.

ZrO_2 and the sol–gel method. The promoted ZrO_2's, however, differ from each other widely in their total basicity and base strength distribution.

DISCUSSION

Catalytic Performance

The present results demonstrate that, depending on the nature of the promoter, the method of catalyst preparation, and the appropriate reaction conditions, ZrO_2 becomes an active, selective, and stable with time-on-stream catalyst in the OCM process. The most effective catalytic system in this class (Na^+–ZrO_2–Cl^-) is obtained by promoting ZrO_2 with Na^+Cl^- via a sol–gel process (Table 3). This indicates that the nature of the alkali promoter and the method of catalyst preparation are two key factors in determining the catalytic behavior of promoted ZrO_2. In addition, the choice of appropriate reaction conditions offers a considerable enhancement in the performance of the catalyst. The promoter effect of Na^+Cl^- in ZrO_2 prepared via the sol–gel method is synergistic, since Na^+Cl^- or ZrO_2 alone exhibit only negligible performances (Table 1). The difference in performance is clearly not a result of surface area, since the latter did not vary much for the pure and the promoted ZrO_2. Moreover, the Na^+–SiO_2–Cl^- or Na^+–TiO_2–Cl^- samples with much higher surface area showed much lower performances than Na^+–ZrO_2–Cl^- (Table 2).

The observation that Li^+–ZrO_2–Cl^-, K^+–ZrO_2–Cl^-, Rb^+–ZrO_2–Cl^-, and Cs^+–ZrO_2–Cl^- (prepared via the sol–gel method) have lower performances than Na^+–ZrO_2–Cl^- (s–g) indicates the importance of the nature of the alkali cation. On the other hand, the superior performance of

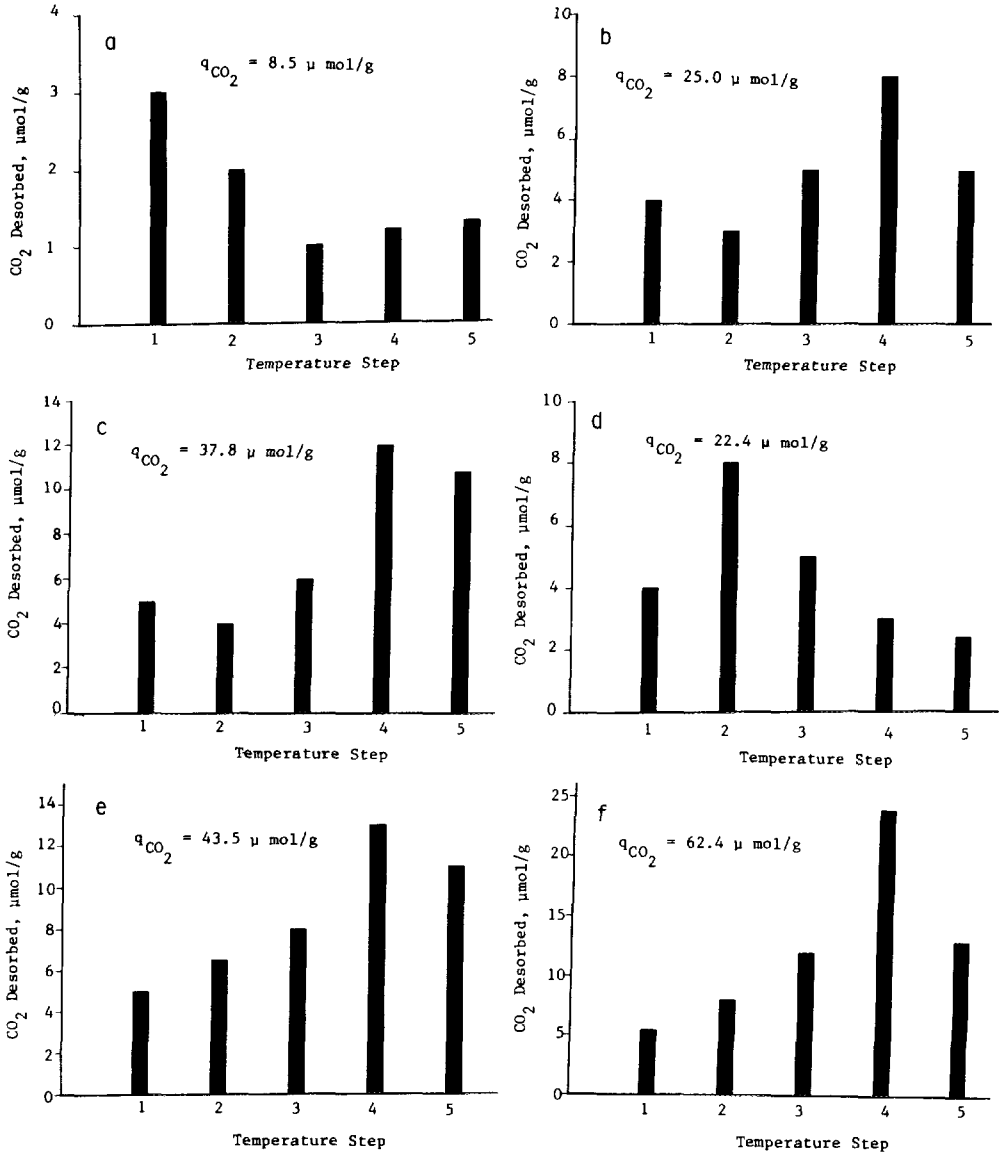

FIG. 9. Stepwise thermal desorption of CO_2 from calcined ZrO_2 and Na^+Cl^--promoted ZrO_2 at 50–850°C (q_{CO_2} = amount of CO_2 chemisorbed at 50°C): (a) ZrO_2, (b) Na^+–ZrO_2–Cl^- (impregnation), (c) Na^+–ZrO_2–Cl^- (gel-precipitation), (d) Na^+–ZrO_2–Cl^- (physical mixing), (e) Na^+–ZrO_2–Cl^- (ion exchange), and (f) Na^+–ZrO_2–Cl^- (sol–gel). Temperature steps: (1) 50–150°C, (2) 150–300°C, (3) 300–500°C, (4) 500–700°C, and (5) 700–850°C.

Na^+Cl^--promoted ZrO_2 to those of $Na^+NO_3^-$-, $Na_2^+CO_3^{-2}$-, and $CH_3COO^-Na^+$-promoted ZrO_2 indicates the important role played by the anion (Cl^-). This is further evidenced by the enhancement exhibited by Na^+–ZrO_2–Cl^- (s–g) upon the addition of carbon tetrachloride (a source of chlorine species) to the feedstream (although the exact nature of the chloride species is not yet known). Apparently, a specific kind of inter-

action between Na^+Cl^- and ZrO_2 gives rise to the enhanced performance.

It is now generally accepted that the generation of methyl radicals from methane by the reactive oxygen species of the oxide catalysts is the crucial step in the OCM process (*1, 23, 24*, and the references therein). In the present study, in addition to the reactive oxygen species there exists a considerable amount of reactive chlorine species which also play an important role in the process. These active chlorine species are present in the catalyst and are additionally produced by the interaction of the Na^+–ZrO_2–Cl^- catalyst with the reactants ($CH_4 + O_2$) and with CTC, when the latter is added to the feedstream. In the absence of the catalyst, the addition of CTC to the feedstream has a negligible effect. It is apparent that, in addition to oxygen, these active chlorine species promote the generation of methyl radicals and this, in turn, enhances the conversion process up to a certain limit. The enhancement of C_2 selectivity over Na^+–ZrO_2–Cl^- (s–g) is possibly due to the blocking by the chlorine species of some of the active sites for complete oxidation to carbon oxides. The noticeable increase in the ethylene-to-ethane ratio in the presence of a chloride catalyst suggests that the chlorine species are also involved in the generation of C_2H_5 radicals from C_2H_6 and ultimately of C_2H_4, as already proposed for other chloride catalysts (*14, 35*).

A major finding of the present study is that the method of catalyst preparation strongly influences the performance of Na^+–ZrO_2–Cl^-, the sol–gel method being the most effective one (Table 3).The different growth kinetics (nucleation, crystal growth, etc.) of each method is responsible for their behavior. The uniqueness of the sol–gel method arises, presumably, from an intimate mixing between Na^+Cl^- and ZrO_2, which is discussed later.

The effect of the operating conditions on the performance of Na^+–ZrO_2–Cl^- (s–g) may shed some light on the possible mechanisms of C_2 hydrocarbons and carbon oxide formations. The increase in the methane conversion and C_2 selectivity with the reaction temperature (Fig. 1) suggests that the formation of methyl radicals by the catalyst is facilitated by high temperatures (>700°C). The total C_2 selectivity passes through a maximum at 750°C but the ethylene-to-ethane ratio continues to increase, which suggests that the oxidation to carbon oxides becomes important at higher temperatures (>750°C), but that the dehydrogenation of ethane to ethylene is facilitated at such temperatures, particularly by chlorine species.

At 750°C the highest CH_4 conversion and C_2 selectivity were obtained over Na^+–ZrO_2–Cl^- (s–g) containing 20% Na^+Cl^-, but further increases in the amount of promoter decreased the performance (Fig. 2). This suggests that there is a cooperation between ZrO_2 and NaCl. If the content of the latter is too high, a too-large fraction of the surface may be covered by NaCl, thus reducing the participation of ZrO_2

The formation of both C_2 hydrocarbons and carbon oxides, although the latter with a low selectivity, at a short pseudo-contact time (Fig. 3) is indicative of the existence of two parallel routes: one which leads to C_2 hydrocarbons and the other to CO_x ($x = 1, 2$), as already noted for many catalysts (*1, 23, 24*). The increase in the C_2 yield and the ethylene-to-ethane ratio up to a certain pseudo-contact time ($0.48\ g \cdot s \cdot ml^{-1}$) is indicative of sequential reactions in which ethylene is formed via a consecutive reaction pathway involving the dehydrogenation of ethane, particularly by chlorine. A further increase in the pseudo-contact time decreases the C_2 yield and the ethylene-to-ethane ratio because at longer residence times in the catalyst bed ethane is more likely to be oxidized than dehydrogenated or ethylene itself is oxidized. The chlorine species which, presumably, block to some extent the oxidation sites on the surface of the catalyst are probably no longer available at long contact times.

The decrease in total C_2 selectivity accompanied by an increase in CO_x ($x = 1, 2$)

selectivity with methane conversion (Fig. 4) is presumably a result of an initial competition between the oxidation of methyl radicals and their coupling to ethane followed by the competition between the dehydrogenation of ethane to ethylene and the oxidation of both hydrocarbons.

The decrease in CH_4 conversion and increases in C_2 selectivity and ethylene-to-ethane ratio with the increase in CH_4 partial pressure (high $CH_4:O_2$ ratio) (Fig. 5) indicate that while the conversion is relatively low at a high CH_4/O_2 ratio, the C_2 selectivity and ethylene-ethane ratio are favored by it. Probably, at a high CH_4/O_2 ratio (low partial pressure of oxygen) the chlorine species facilitates the dehydrogenation of ethane, thereby increasing the ethylene-to-ethane ratio. Unlike the behavior observed with increasing CH_4 partial pressure, the C_2 yield passes through a maximum with increasing oxygen partial pressure (Fig. 6), because at high oxygen partial pressures the equilibrium is shifted in the direction of CO_x, while at low it is shifted in the direction of C_2. An optimum yield exists because a too small amount of oxygen will lead to a small conversion.

The present work demonstrates that the addition of CTC, as a source of chlorine species, into the feedstream has a positive effect only on Na^+Cl^--promoted zirconia. Since in the absence of the catalyst, CTC exhibits a negligible effect, it is likely that additional chlorine species are generated by the interactions between CTC and $Na^+–ZrO_2–Cl^-$. This is consistent with the findings that CTC does not participate in the methane conversion through a purely gas phase process (*30, 35, 40*).

Relationship between Physico-chemical Properties and Catalytic Behavior

The catalytic performances of the $Na^+–ZrO_2–Cl^-$ catalysts, particularly the cooperation among various components, are reflected in their physical and chemical characteristics. The XRD analysis revealed that while $Na^+–ZrO_2–Cl^-$ prepared by impregnation, gel-precipitation, or ion-exchange show similar profiles (Fig. 8), the catalyst prepared by the sol–gel method exhibited some new lines, suggesting that a new phase is formed. More importantly, the sol–gel method ensures the incorporation of a certain amount of Na^+Cl^- into the ZrO_2 matrix, which is reflected in the broadening of some major lines of ZrO_2. The absence of such a line broadening effect in the other catalysts indicates the absence of an intimate mixing between Na^+Cl^- and ZrO_2. The incorporation of Na^+Cl^- into the ZrO_2 matrix has a number of effects on the OCM process; it enhances the CH_4 and O_2 conversions, the C_2 selectivity, the ethylene-to-ethane ratio, and the stability with time-on-stream.

The loss of chlorine is an intrinsic property of the chloride catalysts used in the OCM process (*14, 15, 32*). The $Na^+–ZrO_2–Cl^-$ catalysts are no exception. A noticeable amount of chlorine is lost during calcination followed by a slow decrease during reaction, the amount lost depending on the method of catalyst preparation. Indeed, the XPS results (Table 4) revealed that the concentration of surface chlorine in the calcined $Na^+–ZrO_2–Cl^-$ (s–g) is much higher than those in the samples prepared by gel-precipitation or impregnation. Also, after reaction, the $Na^+–ZrO_2–Cl^-$ (s–g) catalyst contained higher surface concentrations of chlorine than those in the other two catalysts, indicating that the chlorine species are stabilized to a large extent in this system. A similar trend was observed for the surface sodium concentration in $Na^+–ZrO_2–Cl^-$ (s–g), both after calcination and reaction. Most notably, the surface sodium concentration became higher than that of zirconium only in $Na^+–ZrO_2–Cl^-$ (s–g). The Na/Zr was much lower than unity in the samples prepared by gel-precipitation or impregnation. Such an enrichment of the surface with sodium accompanied by an appreciable amount of chlorine exhibits a higher catalytic performance than those prepared by gel-precipitation and impregna-

tion, which have a lower amount of sodium on their surface. Another interesting feature of the sol–gel method is that multiple carbon and oxygen species are present on the Na^+–ZrO_2–Cl^- (s–g) surface, unlike the other catalysts. Perhaps this is associated with the new lines detected in the XRD profile (Fig. 8f). The XRD and XPS results are consistent in that while the former indicates the incorporation of Na^+Cl^- into the ZrO_2 matrix, the latter reveals the stabilization of both sodium and chlorine on the surface enriched with sodium. These factors are likely to contribute to the stability with time-on-stream of Na^+–ZrO_2–Cl^- (s–g), as shown in Fig. 7.

The basicity and base strength distribution studies revealed the presence of site energy distributions on pure ZrO_2 and promoted ZrO_2. The basicity can be attributed to the anions (O^{2-}) exposed at the surface of the catalyst. The base strength (electron pair donor strength) of the surface sites is expected to depend on the effective negative charge on the anions and/or their coordination on the surface (*30*). In view of this, it is likely that the basicity of pure ZrO_2 (which is a weak base) would increase upon promotion with Na^+Cl^- (due to the high electronegativity of chlorine). Indeed, this trend was observed in the present study (Fig. 9) between the unpromoted ZrO_2 and Na^+–ZrO_2–Cl^- prepared by five different methods. The Na^+–ZrO_2–Cl^- (s–g) sample exhibited the highest basicity due, presumably, to the incorporation of a certain amount of Na^+Cl^- into the ZrO_2 matrix (as observed from the XRD analysis) and to the exposure of a noticeable amount of Na^+ and Cl^- on the surface (as evidenced by the XPS studies). The presence of sites of different strengths arises, presumably, from the surface imperfections such as steps, kinks, or corners (*41*).

Thus, the promoting effect of Na^+Cl^- on ZrO_2 is found to emerge from the incorporation of Na^+Cl^- into the ZrO_2 matrix, the exposure of a noticeable amount of Na^+ and Cl^- at the surface and, possibly, from the enhancement of surface basicity and base strength distribution. Obviously, the method of catalyst preparation, namely, the sol–gel process, plays a crucial role in this direction.

CONCLUSION

The following conclusions can be drawn from the present study on the alkali metal compound promoted zirconia catalysts:

(1) An apparently inert ZrO_2 can be made active, selective, and stable with time-on-stream by promoting with alkali metal compounds, notably with alkali metal chlorides. Of all the alkali metal chlorides investigated, Na^+Cl^- was found to be the most effective promoter.

(2) The method of catalyst preparation, the promoter content, and the reaction conditions (temperature, contact time, CH_4/O_2 ratio, and partial pressures of the reactants) have profound effects on the performance of Na^+Cl^--promoted ZrO_2. Out of five different methods used, the sol–gel method was found to produce the most effective Na^+–ZrO_2–Cl^- catalyst, which showed a C_2 yield of 10.6% at a methane conversion of 13.8 mol%. This catalyst also showed a considerable stability with time-on-stream (30 h) at 750°C, unlike other catalysts of the alkali series.

(3) The addition of carbon tetrachloride to the feedstream increased the performance of the Na^+–ZrO_2–Cl^- (s–g) catalyst (up to a C_2 yield of 17.5% at a CH_4 conversion of 22.0 mol%) and its stability with time-on-stream. Such an addition was less effective with other promoted catalysts of the alkali series (also prepared by the sol–gel method).

(4) The presence of the chlorine species is essential, particularly for high C_2 selectivity and ethylene-to-ethane ratio. The concentration of surface chlorine in Na^+–ZrO_2–Cl^- (s–g) is 3–4 times higher than in Na^+–ZrO_2–Cl^- (impregnation) or Na^+–ZrO_2–Cl^- (precipitation), while the sodium concentration is 5–6 times higher than

in the latter two systems. Only in Na^+–ZrO_2–Cl^- (s–g) is the surface sodium concentration found to be higher than that of zirconium.

(5) The promoter effect of Na^+Cl^- on ZrO_2 is likely to be related to the incorporation of Na^+Cl^- into the ZrO_2 matrix, the exposure of an appreciable amount of Na^+ and Cl^- at the surface, and the increase in surface basicity and base strength distribution.

ACKNOWLEDGMENT

We thank Mr. P. Smirniotis for his help with the VAX/VMS program.

REFERENCES

1. Ito, T., Wang, J.-X., Lin, C.-H., and Lunsford, J. H., *J. Am. Chem. Soc.* **107,** 5062 (1985).
2. Aika, K., Moriyama, T., Tasasaki, N., and Iwamatsu, E., *J. Chem. Soc. Chem. Commun.*, 1210 (1986).
3. Carreiro, J. A. S. P., and Baerns, M., *React. Kinet. Catal. Lett.* **35,** 349 (1987).
4. Korf, S. J., Roos, J. A., de Bruijn, N. A., van Ommen, J. G., and Ross, J. R. H., *Catal. Today* **2,** 535 (1988).
5. DeBoy, J. N., and Hicks, R. J., *J. Chem. Soc. Chem. Commun.*, 982 (1988).
6. Iwamatsu, E., Moriyama, T., Takasaki, N., and Aika, K., *J. Catal.* **113,** 25 (1988).
7. Phillip, R., Omata, K., Aoki, A., and Fujimoto, K., *J. Catal.* **134,** 422 (1992).
8. Otsuka, K., Jinno, K., and Morikawa, A., *Chem. Lett.*, 499 (1985).
9. Otsuka, K., and Hatano, M., *J. Catal.* **108,** 252 (1987).
10. Campbell, K. D., Zhang, H., and Lunsford, J. H., *J. Phys. Chem.* **92,** 750 (1988).
11. Gaffney, A. M., U.S. Patent 4,499,323 (1985).
12. Otsuka, K., Liu, Q., and Morikawa, A., *J. Chem. Soc. Chem. Commun.*, 586 (1986).
13. Fujimoto, K., Hashimoto, S., Asami, K., and Tominaga, H., *Chem. Lett.*, 2157 (1987).
14. Burch, R., Squire, G. D., and Tsang, S. C., *Appl. Catal.* **43,** 105 (1988); **46,** 69 (1989); **56,** 219 (1989).
15. Thomas, J. M., Ueda, W., Williams, J., and Harris, K. D. M., *Faraday Discuss. Chem. Soc.* **87,** 33 (1989).
16. Khan, A. Z., and Ruckenstein, E., *Catal. Lett.* **13,** 95 (1992).
17. Burch, R., Chalker, S., Loader, P., Thomas, J. M., and Ueda, W., *Appl. Catal.*, 82, 77 (1992), and the references therein.
18. Otsuka, K., and Komatsu, T., *J. Chem. Soc. Chem. Commun*, 388 (1987).
19. Hatano, M., and Otsuka, K., *Inorg. Chim. Acta* **146,** 243 (1988).
20. Sinev, M. Yu., Korchak, V. N., and Krylov, O. V., *Kinet. Catal.* **27,** 1188 (1987).
21. Sofranko, J. A., Leonard, J. J., and Jones, C. A., *J. Catal.* **103,** 302 (1987).
22. Chan, T. K., and Smith, K. J., *Appl. Catal.* **60,** 13 (1990).
23. Lee, J. S., and Oyama, S. T., *Catal. Rev.-Sci. Eng.* **30,** 249 (1988).
24. Amenomiya, Y., Birss, V. I., Goledzinowski, M., Galuszka, J., and Sanger, A. R., *Catal. Rev.-Sci. Eng.* **32,** 163 (1990).
25. Otsuka, K., Liu, Q., Hatano, M., and Morikawa, A., *Chem. Lett.*, 903 (1986).
26. Hinsen, W., Bytyn, W., and Baerns, M., *in* "Proceedings, 8th International Congress on Catalysis, Berlin, 1984," Vol. 3, p. 581. Verlag Chemie, Frankfurt A. M. Basel, Florida, 1984.
27. Asami, K., Hashimoto, S., Shikada, T., Fujimoto, K., and Tominaga, H., *Chem. Lett.*, 1233 (1986).
28. Meijers, A. C. Q. M., de Jong, A. M., van Gruijthuijsen, L. M. P., and Niemantsverdrict, J. W., *Appl. Catal.* **70,** 53 (1991).
29. Mercera, P. D. L., van Ommen, J. G., Doesburg, E. B. M., Burggraaf, A. J., and Ross, J. R. H., *Appl. Catal.* **71,** 363 (1991).
30. Choudhary, V. R., and Rane, V. H., *J. Catal.* **130,** 411 (1991).
31. Ahmed, S., and Moffat, J. B., *Appl. Catal.* **63,** 129 (1990).
32. Conway, S. J., Wang, D. J., and Lunsford, J. H., *Appl. Catal.* **79,** L1 (1991).
33. Lopez, T., Garcia-Cruz, I., and Gomez, R., J. Catal. **127,** 75 (1991).
34. Hinson, P. G., Clearfield, A., and Lunsford, J. H., *J. Chem. Soc. Chem. Commun.*, 1430 (1991).
35. Khan, A. Z., and Ruckenstein, E., *J. Catal.*, **138,** 322 (1992).
36. Khan, A. Z., and Ruckenstein, E., *Appl. Catal.*, in press.
37. JCPDS Powder Diffraction File. International Center for Diffraction Data, Swarthmore, 1988.
38. Wagner, C. D., Riggs, W. M., Davis, L. E., Moulder, J. F., and Muilenberg, G. E. (Eds.), "Handbook of X-ray Photoelectron Spectroscopy." Perkin–Elmer Corporation, Minnesota, 1978.
39. Miro, E., Sanatamaria, J., and Wolf, E. E., *J. Catal.* **124,** 451 (1990).
40. Ohno, T., and Moffat, J. B., *Catal. Lett.* **9,** 23 (1991).
41. Che, M., and Tench, A. J., *in* "Advances in Catalysis" (D. D. Eley, H. Pines and P. B. Weisz, Eds.), Vol. 31, p. 77. Academic Press, San Diego, 1982.